



ORIGINAL ARTICLE

Open Access



# Experimental study on the embedment strength of smooth dowels inserted in cross-laminated timber narrow side

Weiguo Long<sup>1</sup>, Jiajia Ou<sup>1,2</sup>, Xiaofeng Sun<sup>2\*</sup> , Xinyue Huang<sup>2</sup>, Minjuan He<sup>2</sup> and Zheng Li<sup>2</sup>

## Abstract

The embedment properties of the dowel-type fasteners is a fundamental parameter that can determine the shear resisting performance of the connections utilized in cross-laminated timber (CLT) structures. To investigate the embedment strength of the smooth dowels inserted in CLT narrow side, totally 504 CLT embedment specimens were tested to evaluate the effects of the influencing factors on the embedment strength, which included the loading angle, the embedment angle, the embedment position, the diameter of the dowels, and the gaps between the lumbers. The existing predictive equations of the embedment strength were validated based on the experimental results, and modified empirical equations were proposed for a more accurate prediction on the average embedment strength. It is found that when the loading direction with a loading angle of 90 degree is parallel to the adhesive layer, for the dowels embedded in the core layer and for those embedded between layers, the average embedment strength decreases by 27.89% and by 33.61% with an increase of the diameter from 8 to 24 mm, respectively. When the loading direction is perpendicular to the adhesive layer, the average embedment strength of the smooth dowels with an embedment angle of 90 degree is 85.25–218.96% higher than that of the dowels with an embedment angle of 0 degree. Furthermore, almost no drop can be identified for the embedment strength of the dowels with an embedment angle of 0 degree when the gap exists in their embedment position. A more accurate prediction on the average embedment strength can be achieved based on the modified empirical equations.

**Keywords:** Cross-laminated timber, Smooth dowel, Embedment strength, Influencing factor, Modified empirical equation

## Introduction

Cross-laminated timber (CLT) as a massive engineered wood is composed of several layers of lumber boards stacked crosswise (typically at 90 degrees) and glued together on their wide faces and, sometimes, on their narrow faces as well [1, 2]. Compared to solid wood or glulam, CLT with improved dimensional stability can provide relatively higher in-plane or out-of-plane strength and stiffness, making it typically used as the

shear walls or floor diaphragms in mid- and high-rise timber structures [3–5]. Due to the high strength and stiffness properties of the massive CLT, the lateral performance of the structure that adopts the CLT as primary lateral force resisting members mainly depends on the mechanical properties of the metal connections [6]. Based on their installation locations, the CLT connections can be categorized into the wall-to-foundation joint, wall-to-floor joint, wall-to-wall joint, and floor-to-floor joint [4].

Currently, the most common CLT connections are hold-downs and angle brackets fastened by nails, self-tapping screws or smooth dowels, which are originally introduced from light-weight timber constructions (e.g.,

\*Correspondence: 21310006@tongji.edu.cn

<sup>2</sup> Department of Structural Engineering, Tongji University, Shanghai 200092, China

Full list of author information is available at the end of the article

light-frame wood construction or glulam frame structure) [7, 8]. The embedment strength of the adopted fasteners inserted in CLT is a fundamental parameter that can determine the shear resisting capacity of the CLT connections. Furthermore, compared to glulam or solid wood, the embedment properties of CLT are more complicated due to its unique features. It includes the orthogonal layups, the existing gap between the lumbers, and the reinforcement effect provided by the cross lumbers. Therefore, the CLT embedment strength is actually a system property influenced by several dominant factors, which include the size of the fasteners, the loading angle, the density of CLT, the gap between neighboring lumbers, etc. In addition, it should be noted that the CLT embedment side (e.g., plane side or narrow side) adopted for the connections corresponds to the specific positional relationship between the lumbers and the fasteners. Both the plane side insertion and the narrow side insertion are illustrated in Fig. 1. Therefore, the specific embedment side adopted for the connections can determine the potential factors capable of influencing the CLT embedment strength.

Currently, a large number of studies focus on the embedment behavior of solid wood or glulam [9–12]. Yurrita and Cabrero [10] concluded that the fastener diameter is usually considered as a secondary parameter describing the embedment strength of wood in addition to the wood density. One approach considering the influence of the steel properties was also proposed for the determination of the embedment strength of wood. By contrast, the studies on the more complicated embedment behavior of CLT are relatively limited, and most of them focus on comprehending the influences of the factors on the embedment strength of different fasteners in CLT. Uibel and Blab [13–15] were the first to test

the embedment performance of dowel-type fasteners inserted in both the plane and the narrow sides of CLT. Empirical models considering the CLT layup features were proposed to predict the embedment strength of the fasteners inserted in CLT. Tuhkanen et al. [16] experimentally investigated the influences of the number and the thickness of the lamellas on the embedment strength of fasteners in the case of the CLT plane side insertion. The hardening effect in CLT cross layers was pronounced on larger fastener displacement, resulting in higher embedment strength. For the smooth dowels inserted in CLT plane side, Dong et al. [17] investigated the effects of the lamination thickness, the CLT density, the dowel diameter, and the loading angle on the embedment strength. Overall, each influencing factor could affect the CLT embedment strength significantly, and the influence trends of the four investigated factors were distinctive. Ringhofer et al. [18] reviewed the existing design proposals in form of generic approaches for the embedment strength, and some guidance were suggested. Gikonyo et al. [19] developed a spring model based on the embedment properties of each layer for predicting the embedment behavior of the dowels inserted in CLT plane side. For the CLT with a lamination thickness larger than 20 mm, an ideal agreement was achieved between the numerical behavior and the experimental behavior. Maia et al. [20] evaluated the embedment strength of dowel-type fasteners inserted in CLT plane side, and found the embedment strength depended on the dowel diameter significantly in the case of the loading angle of 0 degree or 90 degree.

In addition, a few studies have focused on the comparison of the embedment properties between the fasteners inserted in the CLT plane side and those inserted in the CLT narrow side. Ringhofer et al. [7] conducted a review on the empirical approaches for predicting the embedment strength of dowel-type fasteners in case of both CLT narrow side insertion and CLT plane side insertion. It was suggested that the distinctions in ductility or failure mode between the fasteners inserted in CLT plane side and the ones inserted in CLT narrow side should be carefully addressed in design. Recently, Dong et al. [21] experimentally investigated the effects of the embedment side and the loading direction on the embedment strength of smooth dowels in CLT. It was found that the transverse and longitudinal layers shared the load jointly when the dowel was inserted in the CLT plane side, resulting in the locking or hardening effect. Therefore, compared to the dowel inserted in the CLT plane side, for that inserted in the CLT narrow side, its failure mode or embedment property was distinctive.

The application of CLT wall or floor panels in construction requires their connections with each other and

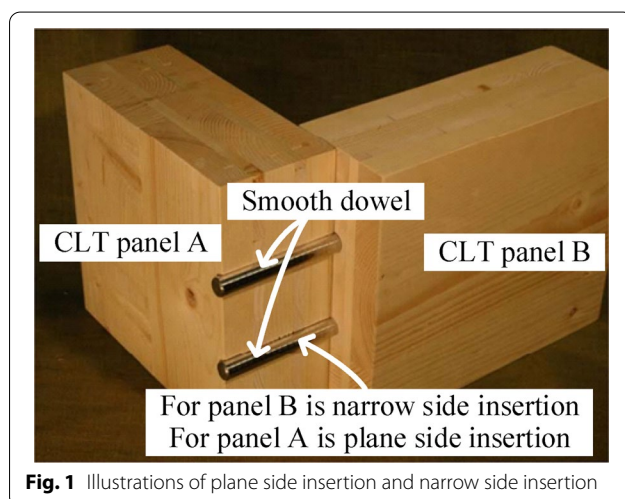


**Fig. 1** Illustrations of plane side insertion and narrow side insertion

with other components of the construction, and for that purpose dowel-type fasteners can be used. For the connections of the CLT walls positioned at an angle, such as wall corners and junctions of partitions and exterior walls, the fasteners are driven into the narrow side (i.e., the edges) of the CLT wall panels to transfer the shear force between the shear walls positioned at an angle. In addition, in a structural system adopting the platform construction method, the CLT walls are connected to the floors above and below the floor level. For the wall-to-floor connections, the fasteners are driven into the narrow side of the CLT wall panels for the transfer of the shear force between the floors and the shear walls, which is induced by the seismic and wind loads. Therefore, it is possible to insert the dowel-type fasteners in the narrow side of the CLT panels. Whereas, in the case of CLT narrow side insertion, the effects of the influencing factors on the embedment strength of the fasteners have not been explicitly addressed, and especially the influence of the gap between the lumbers on the CLT embedment strength still has not been comprehended. Besides, for the smooth dowel inserted in CLT narrow side, the existing limited empirical equations capable of predicting its embedment strength still require comprehensive experiment-based validation. In this study, totally 504 CLT embedment specimens were tested to evaluate the effects of the influencing factors on the embedment strength of the smooth dowels inserted in CLT narrow side, which included the loading angle, the embedment angle, the embedment position, the fastener diameter, and the gap between the lumbers. In this study, the loading angle is defined as the angle between the loading direction and the grain orientation of the CLT face layers, and the embedment angle is defined as the angle between the orientation of the fastener and the grain orientation of the embedment layer. The existing empirical equations for estimating the embedment strength were validated based on the experimental results. Besides, modified equations were also proposed, which could provide a more accurate prediction on the average embedment strength of the dowels inserted in CLT narrow side.

### Equations for embedment strength of dowels inserted in CLT narrow side

Compared to the embedment strength of CLT plane side insertion, the existing empirical equations for potentially predicting the embedment strength of CLT narrow side insertion are relatively limited, which are introduced in the following. The notations relative to the density that are used in the equations are listed herein: (1)  $\rho_{12}$  ( $\text{g}/\text{cm}^3$ ) is the measured density based on mass and volume of CLT with 12% moisture content according to European code EN 1995-1-2 [22]; (2)  $\rho_{12,k}$  ( $\text{g}/\text{cm}^3$ ) is the

characteristic density based on mass and volume of CLT with 12% moisture content according to EN 1995-1-2 [22]; (3)  $G$  ( $\text{g}/\text{cm}^3$ ) is the characteristic relative density based on oven-dry mass and volume according to Canadian code CSA O86 [23]; (4)  $G_0$  ( $\text{g}/\text{cm}^3$ ) is the measured relative density for the species or species group based on oven-dry mass and volume according to CSA O86 [23].

Based on the studies from Kennedy et al. [24] and NDS [25], the density defined in the European code can be transformed into the relative density defined in the Canadian or American code based on the following adjustments: (1) converting the average density at 12% moisture content to the characteristic density at 15% moisture content by multiplying by 0.89; (2) converting the characteristic density at 15% moisture content to the oven-dry relative density by multiplying by 1.075; (3) converting the mean relative density to the oven-dry characteristic density by multiplying by 0.8.

### Equations by Uibel and Blab

Uibel and Blab tested the embedment properties of the smooth dowels inserted in CLT narrow side and proposed an empirical mode for predicting the embedment strength [13–15]. It can be expressed by Eqs. (1) and (2), in which, the average and the characteristic values of the embedment strength,  $f_{\theta,ave,UB,nar}$  (MPa) and  $f_{\theta,k,UB,nar}$  (MPa), are dependent on both the diameter of fasteners and the density of CLT. The  $d$  (mm) is the nominal diameter of the dowels:

$$f_{\theta,ave,UB,nar} = 26.31 \cdot (1 - 0.017d) \cdot \rho_{12}^{0.91} \quad (1)$$

$$f_{\theta,k,UB,nar} = 23.36 \cdot (1 - 0.017d) \cdot \rho_{12,k}^{0.91} \quad (2)$$

### Equations from the code CSA O86

The empirical model from the CSA O86 [23] can be potentially applied to the estimation of the embedment strength of smooth dowels in the case of CLT narrow side insertion. In that model, the embedment strength is considered dependent on the diameter of fasteners, the density of CLT, and the loading angle relative to the grain orientation of the individual embedment layer of CLT. The empirical model can be expressed by Eqs. (3) and (4), in which,  $f_{\theta,ave,CSA,nar}$  (MPa) and  $f_{\theta,k,CSA,nar}$  (MPa), respectively, represent the average value and the characteristic value of the embedment strength estimated based on the CSA O86 [23].  $\theta_e$  represents the loading angle relative to the grain of the individual embedment layer, which can be adopted as 0 degree and 90 degree for the embedment strength parallel to and perpendicular to the grain of the embedment layer, respectively. It should be noted that when the smooth dowel inserted in CLT narrow side was

positioned between CLT layers, the  $\theta_e$  was adopted as the loading angle relative to the grain orientation of the CLT core layer in this study:

$$f_{\theta,ave,CSA,nar} = \frac{0.9 \times 82\rho_{12}(1 - 0.01d)}{0.9 \times 2.27 \sin^2 \theta_e + \cos^2 \theta_e} \quad (3)$$

$$f_{\theta,k,CSA,nar} = \frac{0.9 \times 50G(1 - 0.01d)}{0.9 \times 2.27 \sin^2 \theta_e + \cos^2 \theta_e} \quad (4)$$

## Materials and methods

### General plan

For the studied three-layer CLT, the angle between the loading direction and the grain orientation of the CLT face layers was defined as the loading angle  $\theta$ ; besides, the angle between the orientation of the dowel and the grain orientation of the embedment layer (i.e., core layer of CLT) was defined as the embedment angle  $\beta$ . For the smooth dowels inserted in CLT narrow side, based on the loading direction, the  $\theta$ , and the  $\beta$ , totally four cases should be considered when estimating the embedment strength, as shown in Fig. 2. They are, namely, the loading direction is parallel to the adhesive layer with a  $\theta$  of 0 degree (dir 1), the loading direction is parallel to the adhesive layer with a  $\theta$  of 90 degree (dir 2), the loading direction is perpendicular to the adhesive layer with a  $\beta$  of 0 degree (dir 3), and loading direction is perpendicular to the adhesive layer with a  $\beta$  of 90 degree (dir 4), respectively.

In this study, all the three-layer CLT embedment specimens with a total thickness  $t$  of 105 mm were divided into group A and group B. All the CLT specimens were manufactured using the adhesive of phenol resorcinol formaldehyde (PRF), which was a conventional wood laminating adhesive. For the embedment specimens of the group A with the loading direction parallel to the adhesive layer (i.e., directions 1 and 2), the influence of the dowel nominal diameter  $d$  was considered. Besides, it is possible to position the smooth dowel between the core layer and the face layer when it is inserted in CLT narrow side, namely, the influence of the adhesive layer of CLT on its embedment strength was also considered for the specimens of the group A. Therefore, when the loading direction was parallel to the adhesive layer, subgroups

1 to 8 of CLT embedment specimens were tested to investigate the effects of the  $\theta$ , the  $d$ , and the adhesive layer of CLT on the embedment strength of the smooth dowels inserted in CLT narrow side. In addition, for the embedment specimens of the group B with the loading direction perpendicular to the adhesive layer (i.e., directions 3 and 4), subgroups 9 to 16 of CLT embedment specimens were tested to investigate the effects of the  $d$ , the gap between the neighboring lumbers within the core layer, and the embedment angle  $\beta$  on their embedment strength. For the embedment tests conducted in the group A or the group B, the  $d$  of the smooth dowels was adopted as 8 mm and 24 mm, respectively. The details of the cubic CLT embedment specimens from the subgroups 1 to 16 are listed in Table 1. Totally 504 CLT embedment specimens were tested, and the replicates of the specimens tested for each subgroup are also listed in Table 1. The final replicates tested in each subgroup were determined based on an iterative calculation method recommended by EN 14358 [26]. During the iterative calculation method, the final replicates depend on the estimated coefficient of variation (COV) of the measured embedment strength per subgroup. Additional cubic specimens should be supplemented to the embedment tests until the estimated COV is less than its upper limitation that is corresponding to a specific sample size.

### Materials

All the cubic CLT embedment specimens were sampled from the non-edge-glued three-layer CLT panels with a total thickness of 105 mm, which were manufactured from the No.2-grade Spruce-pine-fir (SPF) lumbers [27] with a cross-sectional dimensions of 140 mm  $\times$  35 mm (width  $\times$  thickness). The average density of these CLT panels was 494 kg/m<sup>3</sup> with a COV of 4.3%. Based on the code EN 383 [28], it is recommended that the  $d$  of the dowel-type fasteners should be less than one quarter of the embedment length  $l$ . In this study, the  $l$  was adopted as 140 mm and 70 mm for the smooth dowels with a  $d$  of 24 mm and those with a  $d$  of 8 mm, respectively. Therefore, for the smooth dowels with a  $d$  of 24 mm and those with a  $d$  of 8 mm, the CLT embedment specimens with a plane size of 140 mm  $\times$  140 mm and those with a plane size of 140 mm  $\times$  70 mm were used to test their embedment strength, respectively. The embedment length

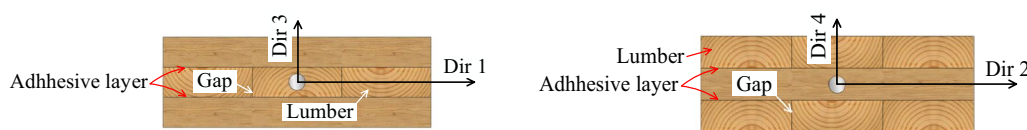


Fig. 2 Smooth dowel inserted in CLT narrow side

**Table 1** Details of cubic CLT embedment specimens

Subgroup	Label	$d$ (mm)	$\theta$ (degree)	$\beta$ (degree)	Adhesive layer or gap	Replicates
1	A- $\theta=0$ -24-NA	24	0	0	No	16
2	A- $\theta=90$ -24-NA	24	90	90	No	20
3	A- $\theta=0$ -24-A	24	0	–	Yes	24
4	A- $\theta=90$ -24-A	24	90	–	Yes	43
5	A- $\theta=0$ -8-NA	8	0	0	No	41
6	A- $\theta=90$ -8-NA	8	90	90	No	29
7	A- $\theta=0$ -8-A	8	0	–	Yes	40
8	A- $\theta=90$ -8-A	8	90	–	Yes	39
9	B- $\beta=0$ -24-NG	24	–	0	No	37
10	B- $\beta=90$ -24-NG	24	–	90	No	20
11	B- $\beta=0$ -24-G	24	–	0	Yes	18
12	B- $\beta=90$ -24-G	24	–	90	Yes	22
13	B- $\beta=0$ -8-NG	8	–	0	No	36
14	B- $\beta=90$ -8-NG	8	–	90	No	43
15	B- $\beta=0$ -8-G	8	–	0	Yes	35
16	B- $\beta=90$ -8-G	8	–	90	Yes	41

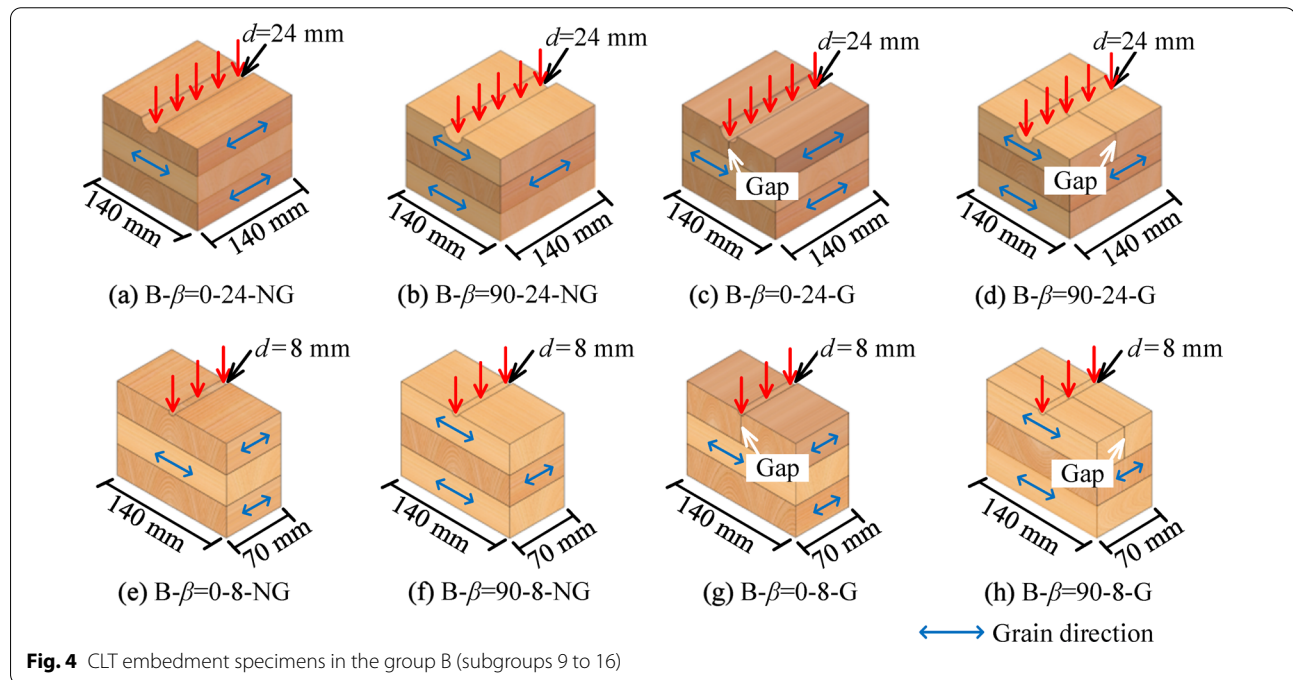
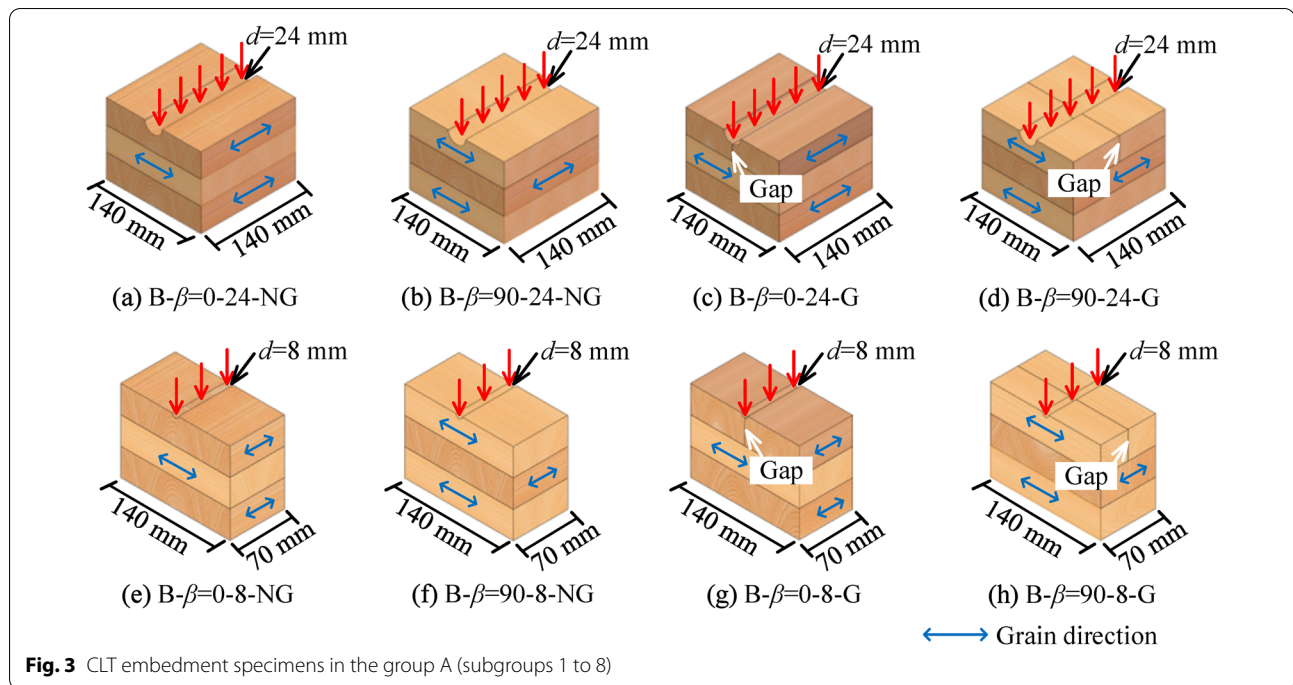
was different for the smooth dowels with a  $d$  of 8 mm and those with a  $d$  of 24 mm. It should be admitted that such an arrangement would induce the influence from the variation of the embedment length on the measured embedment strength. Whereas, based on the experimental studies conducted by Blaß and Uibel [29] and Xu et al. [30], it was indicated that the influence of the embedment length on the embedment strength was much less compared to that of the  $d$ . Therefore, the influence of embedment length on the strength was not considered in this paper but should be studied further to quantify the influence of changes in embedment length on the embedment strength of the smooth dowels inserted in CLT. All the CLT embedment specimens were placed in the constant temperature and humidity chamber (20 °C and 65% relative humidity) for almost 2 weeks to reach an average moisture content of 12% prior to the embedment tests. The configurations of the CLT embedment specimens in the subgroups 1 to 8 and those of the CLT embedment specimens in the subgroups 9 to 16 are illustrated in Figs. 3 and 4, respectively. Based on the ASTM D5764 [31], the half hole in each embedment specimen should be predrilled with a diameter 1.6 mm larger than the  $d$  of the tested dowel. Taking the smooth dowel with a  $d$  of 24 mm as an example, a pair of cubic embedment specimens were put together with their embedment sides closely adjacent, and then a 25.6-mm-diameter hole was drilled in the center of both embedment specimens, forming a predrilled half hole with an identical diameter in each embedment specimen.

#### Embedment test method

Compared to the complete-hole test configuration from the EN 383 [28], the half-hole test configuration from the ASTM D5764 [31] for the embedment strength is less susceptible to the bending of the dowels [32]. Therefore, all the embedment tests in this study were conducted based on the half-hole test configuration, as shown in Fig. 5. Since the displacement from the loading head was found much close to that measured from the linear variable differential transducers (LVDTs) mounted at both sides of the specimen, the displacement from the loading head was adopted as the embedment displacement for simplification. One Q235 steel plate with a thickness equal to the  $d$  of the dowel was connected to the loading head to simulate the laterally loaded smooth dowel embedded in the cubic CLT specimen. The embedment specimens were loaded with a constant loading rate of 1.0 mm/min, and the embedment test was terminated once the peak embedment load or the embedment displacement equal to  $0.5d$  was reached.

The experimental embedment strength  $f_e$  can be calculated based on Eq. (5), in which  $P_y$  represents the 5% diameter offset load obtained based on the method from the ASTM D5764 [31], and  $l$  represents the embedment length. The characteristic value of the experimental embedment strength  $f_{e,k}$  was calculated based on EN 14358 [26]:

$$f_e = \frac{P_y}{l \cdot d}. \quad (5)$$



## Results and discussion

### Embedment behavior and failure mode

The related values of the experimental embedment strength of each subgroup are summarized and listed in Table 2, which include the maximum embedment strength  $f_{e,max}$ , the minimum embedment strength  $f_{e,min}$ ,

the average embedment strength  $f_{e,ave}$ , the COVs, and the characteristic embedment strength  $f_{e,k}$ . For the group A or the group B, when the  $d$  is enhanced from 8 to 24 mm, the variation in the corresponding embedment strength  $f_e$  is not significant. For instance, for the group A,  $f_{e,ave}$  of the dowels with an 8-mm  $d$  is in the range of

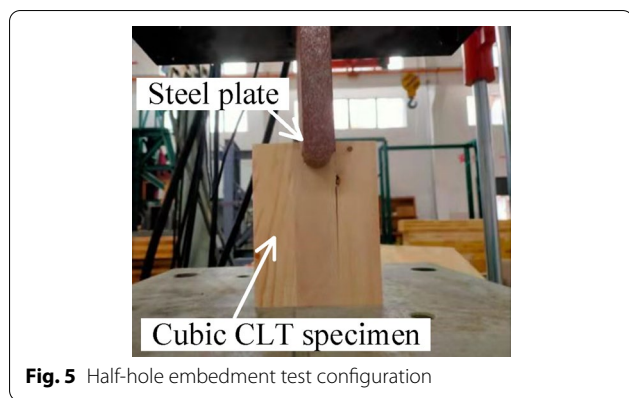


**Fig. 5** Half-hole embedment test configuration

5.84–38.55 MPa (Table 2), and that of the dowels with a 24-mm  $d$  is in the range of 5.79–27.80 MPa (Table 2).

For the average force–displacement curves of the specimens in subgroups 2 to 4 and for those of the specimens in subgroups 6 to 8, the embedment force declines when the displacement exceeds a critical value, as shown in Fig. 5a, b. Whereas, for the average force–displacement curves of the specimens in subgroups 9 to 16, no degradation of the embedment force can be observed during the loading process, as shown in Fig. 5c, d. It indicates that a significant difference in ductility exists in the embedment behaviors of the dowels inserted in CLT narrow side between the case of the loading direction parallel to the adhesive layer and that of the loading direction perpendicular to the adhesive layer. The loading angle  $\theta$ , the embedment angle  $\beta$ , the adhesive layer, and the gap between the lumbers have a statistically

significant influence on the embedment strength of the dowels in CLT, and the influence trends of them on the embedment strength are different. A more detailed analysis on the effects of these influencing factors on the embedment strength will be conducted in the following.

For the specimens in subgroups 1 to 4 and those in subgroups 6 to 8, in their average force–displacement curves, the embedment force declines when the displacement exceeds a critical value. The embedment force corresponding to that critical displacement was obtained as the ultimate embedment force  $F_u$  of the CLT embedment specimens. As for the specimens in the other subgroups, no degradation of the embedment force can be observed in their average force–displacement curves (Fig. 6). The maximum embedment force  $F_{max}$  was obtained from the average force–displacement curves of those CLT embedment specimens.  $F_u$  or  $F_{max}$  obtained from the average force–displacement curve of the specimens per subgroup is listed in Table 3. The embedment specimens in the subgroups 9 to 16 were tested using the smooth dowels with a  $d$  of 24 mm. For the specimens in the subgroups 9 to 16, no significant decrease of the embedment force were observed in their force–displacement curves, although slight crushing might occur in some specimens during the loading process. Therefore, based on the requirements from ASTM D5764 [31], it was determined that all the specimens in the subgroups 9 to 16 were loaded to a displacement equal to  $0.5d$  (i.e., 12 mm). The average force–displacement curves of those embedment specimens are shown in Fig. 6d, and the embedment

**Table 2** Experimental embedment strength of all the subgroups

Subgroup	Label	Replicates	$f_{e,max}$ (MPa)	$f_{e,min}$ (MPa)	COV (%)	$f_{e,ave}$ (MPa)	$f_{e,k}$ (MPa)
1	A- $\theta=0$ -24-NA	16	7.98	4.77	12.0	5.79	3.73
2	A- $\theta=90$ -24-NA	20	34.59	18.91	13.9	27.80	18.42
3	A- $\theta=0$ -24-A	24	21.94	13.51	13.4	16.90	12.60
4	A- $\theta=90$ -24-A	43	16.85	5.96	25.2	11.06	5.97
5	A- $\theta=0$ -8-NA	41	8.70	3.97	19.8	5.84	3.72
6	A- $\theta=90$ -8-NA	29	49.41	27.99	18.9	38.55	24.91
7	A- $\theta=0$ -8-A	40	25.64	13.03	18.3	18.17	12.07
8	A- $\theta=90$ -8-A	39	24.48	10.23	21.7	16.66	10.02
9	B- $\beta=0$ -24-NG	37	8.27	3.62	22.9	5.82	3.37
10	B- $\beta=90$ -24-NG	20	15.47	8.29	18.3	11.75	7.68
11	B- $\beta=0$ -24-G	18	7.69	4.53	13.5	5.83	3.54
12	B- $\beta=90$ -24-G	22	13.23	8.05	15.0	10.80	7.60
13	B- $\beta=0$ -8-NG	36	8.27	4.62	19.9	6.01	3.81
14	B- $\beta=90$ -8-NG	43	23.68	14.88	12.1	19.17	14.95
15	B- $\beta=0$ -8-G	35	9.98	4.53	25.5	6.77	3.61
16	B- $\beta=90$ -8-G	41	22.58	10.97	13.0	17.70	13.50

$f_{e,k}$  was calculated based on the method from EN 14358 [26]

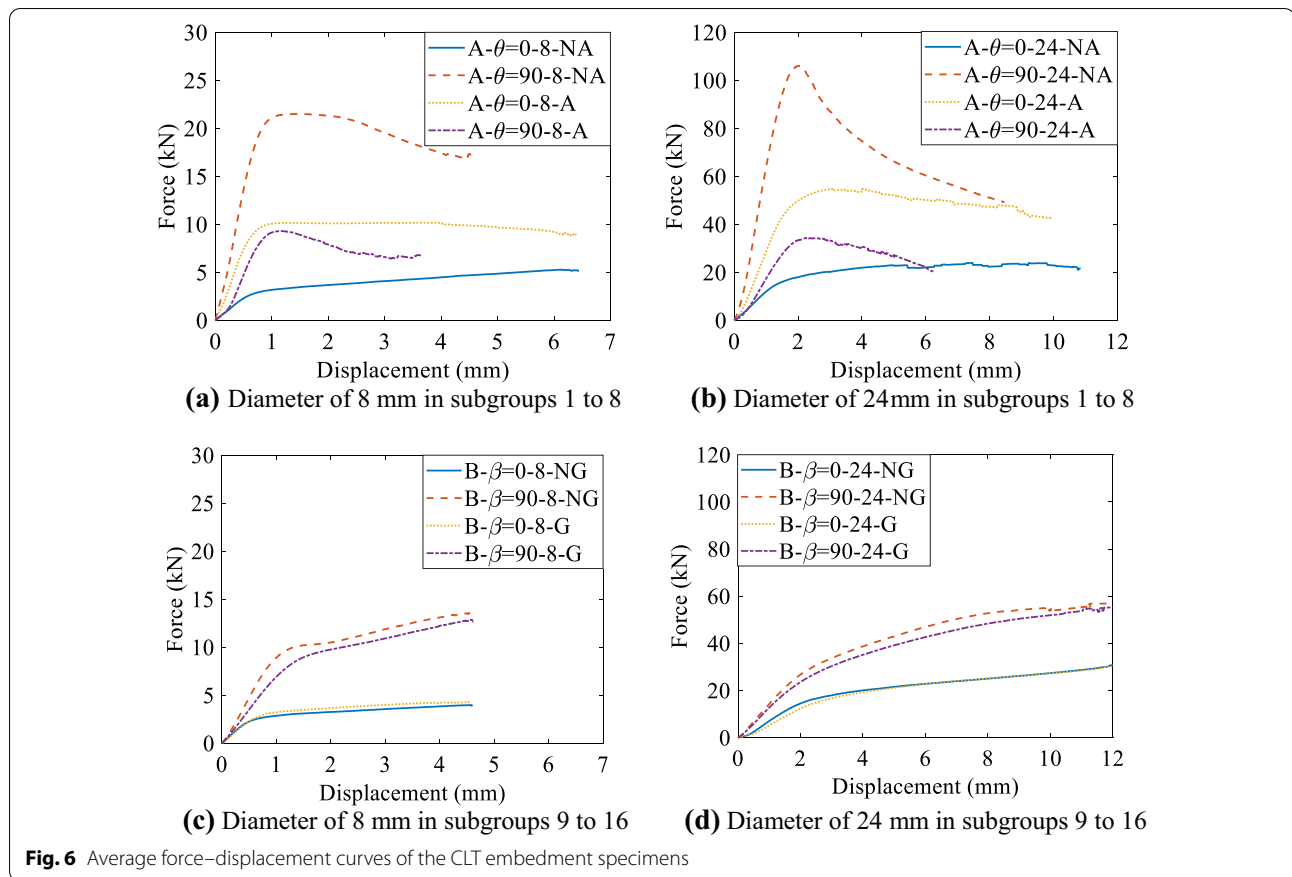


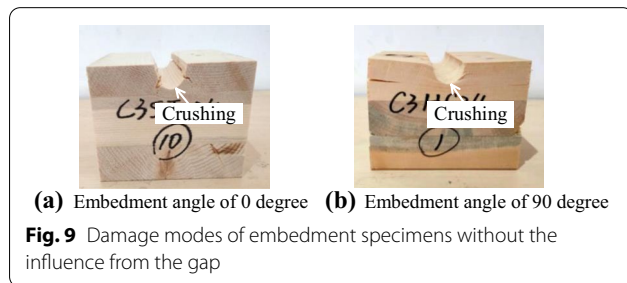
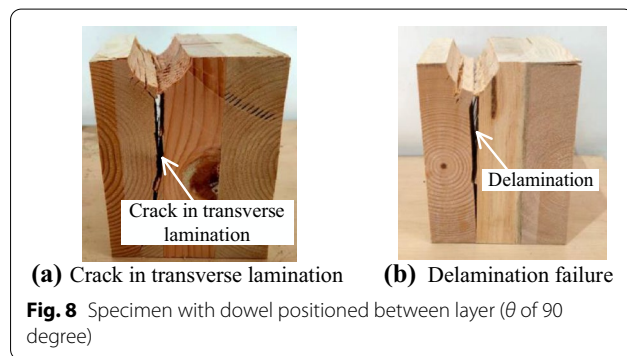
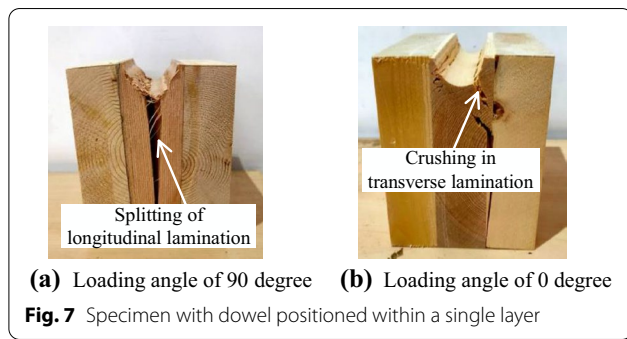
**Table 3**  $F_u$  or  $F_{max}$  obtained from the average force–displacement curve

Subgroup	Label	Force	Value (kN)	Increasing ratio
1	A- $\theta=0$ -24-NA	$F_u$	24.00	4.53
2	A- $\theta=90$ -24-NA	$F_u$	106.03	4.94
3	A- $\theta=0$ -24-A	$F_u$	54.73	5.39
4	A- $\theta=90$ -24-A	$F_u$	34.37	3.69
5	A- $\theta=0$ -8-NA	$F_{max}$	5.30	–
6	A- $\theta=90$ -8-NA	$F_u$	21.47	–
7	A- $\theta=0$ -8-A	$F_u$	10.15	–
8	A- $\theta=90$ -8-A	$F_u$	9.30	–
9	B- $\beta=0$ -24-NG	$F_{max}$	31.47	7.91
10	B- $\beta=90$ -24-NG	$F_{max}$	56.83	4.15
11	B- $\beta=0$ -24-G	$F_{max}$	30.86	7.18
12	B- $\beta=90$ -24-G	$F_{max}$	55.17	4.27
13	B- $\beta=0$ -8-NG	$F_{max}$	3.98	–
14	B- $\beta=90$ -8-NG	$F_{max}$	13.67	–
15	B- $\beta=0$ -8-G	$F_{max}$	4.30	–
16	B- $\beta=90$ -8-G	$F_{max}$	12.91	–

force corresponding to the displacement of 12 mm was obtained as  $F_{max}$  of the specimens.

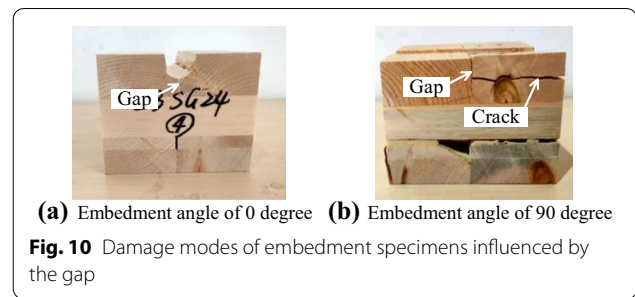
For the specimens in subgroups 2 to 4 and those in subgroups 6 to 8, the increasing ratio between  $F_u$  of the 24-mm- $d$  dowels to that of the 8-mm- $d$  dowels is within the range of 3.69–5.39. For the specimens in subgroups 9 to 16, when the  $\beta$  is 0 degree, the increasing ratio between  $F_{max}$  of the 24-mm- $d$  dowels to that of the 8-mm- $d$  dowels is within the range of 7.18–7.91. By contrast, when the  $\beta$  is 90 degree, the increasing ratio between  $F_{max}$  of the 24-mm- $d$  dowels to that of the 8-mm- $d$  dowels is within the range of 4.15–4.27. It should be noted the influence of the embedment length on the embedment force was not considered, which should be studied further to quantify the influence of changes in embedment length on the embedment force of the dowels in CLT.

The failure mode of the embedment specimens from subgroups 1 to 8 depends on the specific embedment location of the dowels in CLT. When the embedded smooth dowel was positioned within the CLT core layer, for the embedment specimen with a  $\theta$  of 90



degree, splitting failure occurred within its longitudinal core lamination; for the embedment specimen with a  $\theta$  of 0 degree, its transverse core lamination was crushed, as illustrated in Fig. 7. When the embedded smooth dowel was positioned between the CLT layers, preliminary crack formed and propagated in the CLT transverse lamination; besides, delamination failure might occurred along the adhesive layer of a small part of embedment specimens, as illustrated in Fig. 8.

For the embedment specimens with the loading direction perpendicular to the adhesive layer of the CLT, when gap did not exist in the embedment position, crushing failure occurred in the embedment lamination of the specimens in case of a  $\beta$  of 0 degree or 90 degree, as shown in Fig. 9. When the gap between lumbers



existed in the embedment position of the dowel, in case of a  $\beta$  of 90 degree, preliminary crack formed and propagated near the edge sides of the embedment specimens, which was induced by the warpage of the CLT embedment lamination, as shown in Fig. 10b.

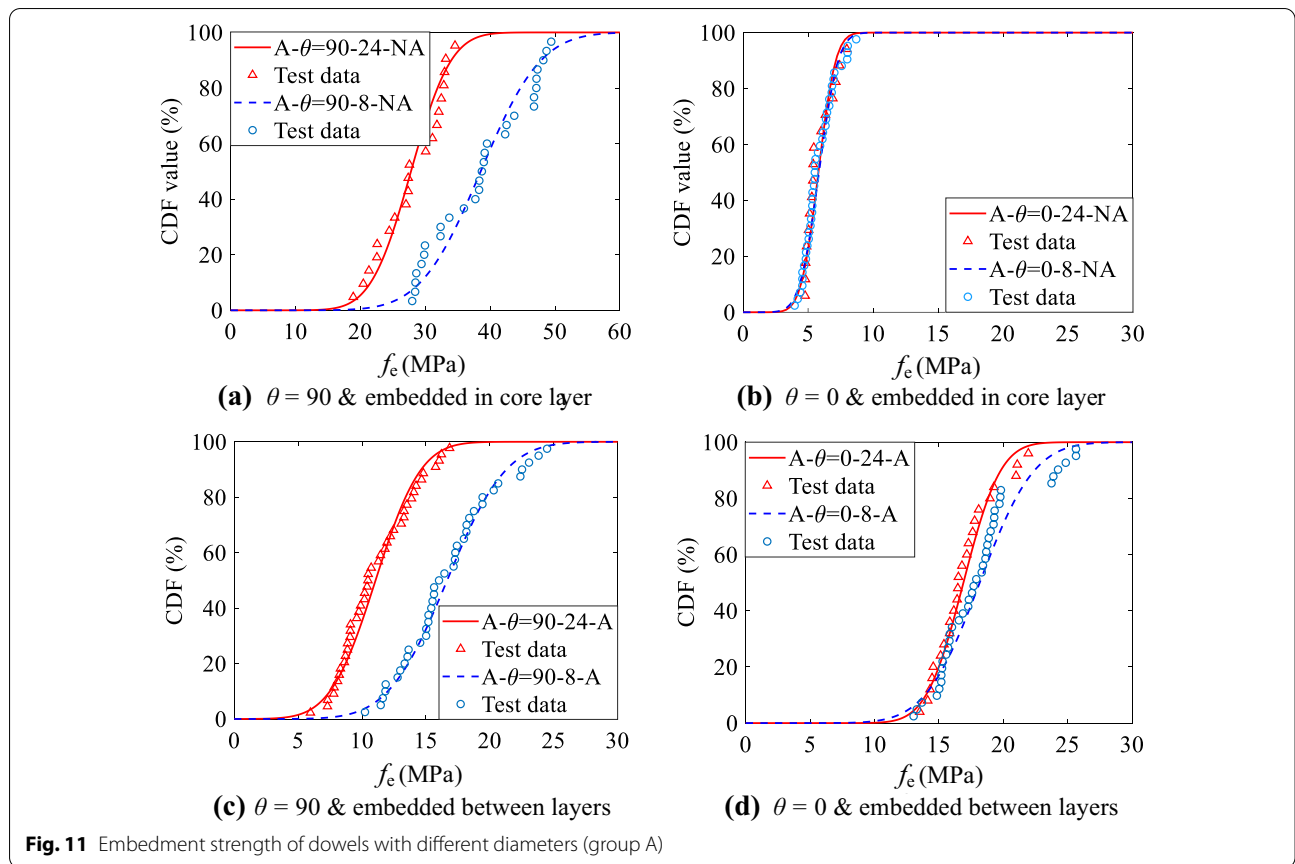
### Influencing factors on the embedment strength

#### Diameter of dowel

The curves formed based on the empirical cumulative distribution functions (CDFs) of the embedment strength  $f_e$  were adopted to analyze the effects of the influencing factors on  $f_e$ . The influence from the diameter of the smooth dowels  $d$  on the embedment strength was investigated for the CLT embedment specimens in the group A and for those in the group B, respectively. For the embedment tests conducted in the subgroups 1 to 8, whether the  $d$  had an effect on  $f_e$  depended on the value of  $\theta$ . As shown in Fig. 11a, c, in case of the  $\theta$  adopted as 90 degree, when the  $d$  is enhanced from 8 to 24 mm,  $f_{e,ave}$  decreases by 27.89% and 33.61% (Table 2) for the dowels embedded in the core layer and for those embedded between layers, respectively. Whereas, in case of the  $\theta$  adopted as 0 degree,  $f_e$  of the dowels with a  $d$  of 8 mm is similar to that of the dowels with a  $d$  of 24 mm, as shown in Fig. 11b, d.

For the embedment tests conducted in the subgroups 9 to 16, whether the  $d$  had an effect on the embedment strength  $f_e$  depended on the value of  $\beta$ . As shown in Fig. 12a, c, in case of the  $\beta$  adopted as 90 degree, when the  $d$  is enhanced from 8 to 24 mm,  $f_{e,ave}$  decreases by 38.71% and 43.70% (Table 2) for the dowels that are not influenced by the gap and for those influenced by the gap, respectively. Whereas, in case of the  $\beta$  adopted as 0 degree,  $f_e$  of the dowels with a  $d$  of 8 mm is similar to that of the dowels with a  $d$  of 24 mm, as shown in Fig. 12b, d.

Overall, for the embedment specimens with the loading direction parallel to the adhesive layer, when the  $\theta$  is 90 degree, the embedment strength decreases with an increasing of the diameter of the dowels, as shown in Fig. 11a, c. For the embedment specimens with the loading direction perpendicular to the adhesive layer, when



the  $\beta$  is 90 degree, the embedment strength decreases with an increasing of the diameter of the dowels, as shown in Fig. 12a, c. Similar findings were also reported in the references [13–15, 17, 29]. It is because the embedment area of the CLT specimens covered by the dowels is enhanced when the  $d$  increases. Due to the size effect, more intrinsic defects would be contained and the experimental embedment strength is weakened. Considering the influence of the embedment length on the embedment strength was much less compared to that of the diameter of the dowels [29, 30], the influence of the embedment length on the embedment strength was not considered in this study, which should be further investigated in the future.

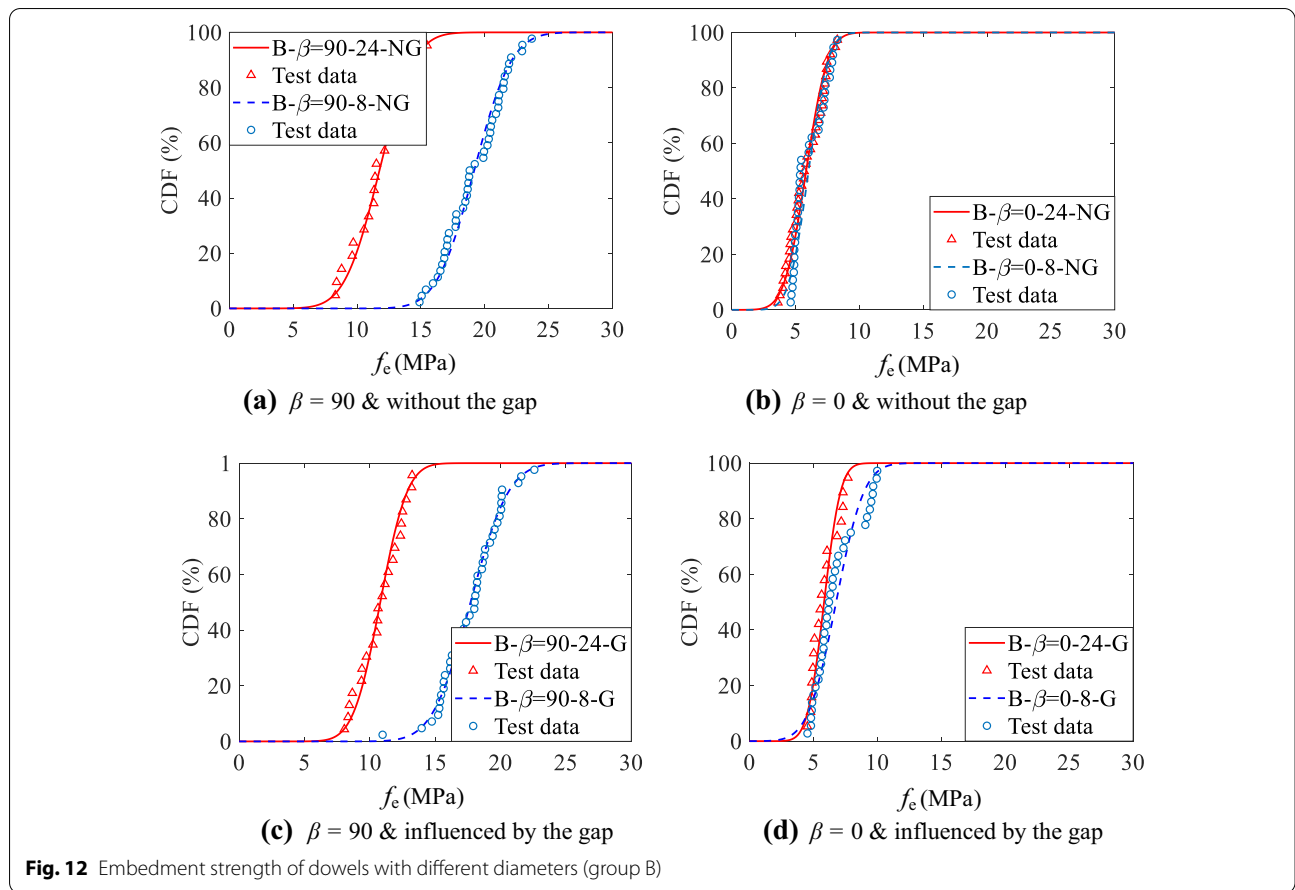
**Loading angle**

When embedded in the CLT core layer,  $f_e$  of the dowels laterally loaded with a  $\theta$  of 90 degree is significantly higher, compared to the dowels loaded with a  $\theta$  of 0 degree, as shown in Fig. 13a, b. It is due to the obvious reason that the grain orientation of the embedded core layer is parallel to the loading direction in the case of the 90-degree  $\theta$ , and in the case of the 0-degree  $\theta$ , the grain orientation of the embedded core layer is perpendicular

to the loading direction. By contrast, when embedded between the CLT layers,  $f_{e,ave}$  of the dowels loaded with a  $\theta$  of 90 degree are 34.55% smaller and 8.31% smaller (Table 2) than that of the dowels loaded with a  $\theta$  of 0 degree for the  $d$  of 24 mm and for the  $d$  of 8 mm, respectively (Fig. 13c, d). It is because the CLT with the dowels loaded with a  $\theta$  of 0 degree is composed of two longitudinal face layers and one transverse core layer. Its in-plane compressive strength is higher than that of the CLT with the dowels loaded with a 90-degree  $\theta$ , which is composed of two transverse face layers and one longitudinal core layer. Therefore, for the smooth dowel positioned between the face layer and the core layer, the  $f_e$  actually belonging to the local in-plane compressive strength of CLT is higher in the case of the  $\theta$  adopted as 0 degree.

**Adhesive layer of CLT**

For the embedment specimens in subgroups 1 to 8, when the  $\theta$  is adopted as 90 degree,  $f_e$  of the dowels embedded within the CLT longitudinal core layer is significantly higher than that of the dowels embedded between the face layer and the core layer, as shown in Fig. 14a, c. Whereas, when the  $\theta$  is adopted as 0 degree,  $f_e$  of the dowels embedded between the face layer and the core



layer is significantly higher than that of the dowels embedded within the CLT transverse core layer, as shown in Fig. 14b, d. It is because the embedment area (i.e.,  $l \times d$ ) equally covers the longitudinal layer and the transverse layer for the dowel positioned between the CLT layers, and the corresponding  $f_e$  can be approximated as the average value of the parallel-to-grain compressive strength and the perpendicular-to-grain compressive strength of the lumber. Besides, comparison between the experimental embedment strength and the compressive strength of the lumber was conducted. The material data of the No. 2-grade SPF lumber was provided by the CLT manufacturer. The average compressive strength of the lumber in the parallel-to-grain direction  $f_{lc,0}$  and that of the lumber in the perpendicular-to-grain direction  $f_{lc,90}$  were adopted as 28.7 MPa with a COV of 9.2% and 5.8 MPa with a COV of 10.4%, respectively. Therefore, the average value of  $f_{lc,0}$  and  $f_{lc,90}$  was 17.25 MPa. For the specimens in the four groups with the dowels embedded between layers (i.e., A- $\theta$ =90-24-A, A- $\theta$ =90-8-A, A- $\theta$ =0-24-A, and A- $\theta$ =0-8-A), their  $f_{e,ave}$  was within the range of 11.06–18.17 MPa. The average value of 17.25 MPa was similar to  $f_{e,ave}$  of the specimens in the

four aforementioned groups, which was within the range of 11.06–18.17 MPa.

#### Embedment angle

For the CLT embedment specimens in the subgroups 9 to 16,  $f_{e,ave}$  of the laterally loaded dowels with a  $\beta$  of 90 degree is 85.25–218.96% higher (Table 2) than that of the dowels with a  $\beta$  of 0 degree. It indicates that the  $\beta$  is the most dominant factor affecting  $f_e$  of the dowels inserted in CLT narrow side in case of the loading direction perpendicular to the adhesive layer. Besides, the distinction between  $f_e$  of the dowels with a  $\beta$  of 90 degree and that of the dowels with a  $\beta$  of 0 degree is more pronounced when the  $d$  decreases from 24 to 8 mm, as shown in Fig. 15. It is because when the  $\beta$  is 90 degree, the orientation of the dowel is perpendicular to the grain orientation of the embedment layer. More wood fibers of the embedment layer are subjected to the embedment force, and the number of the embedded wood fibers is actually determined by the length of the dowels. By contrast, when the  $\beta$  is 0 degree, the orientation of the dowel is parallel to the grain orientation of the embedment layer, and less wood fibers of the embedment layer are subjected to the

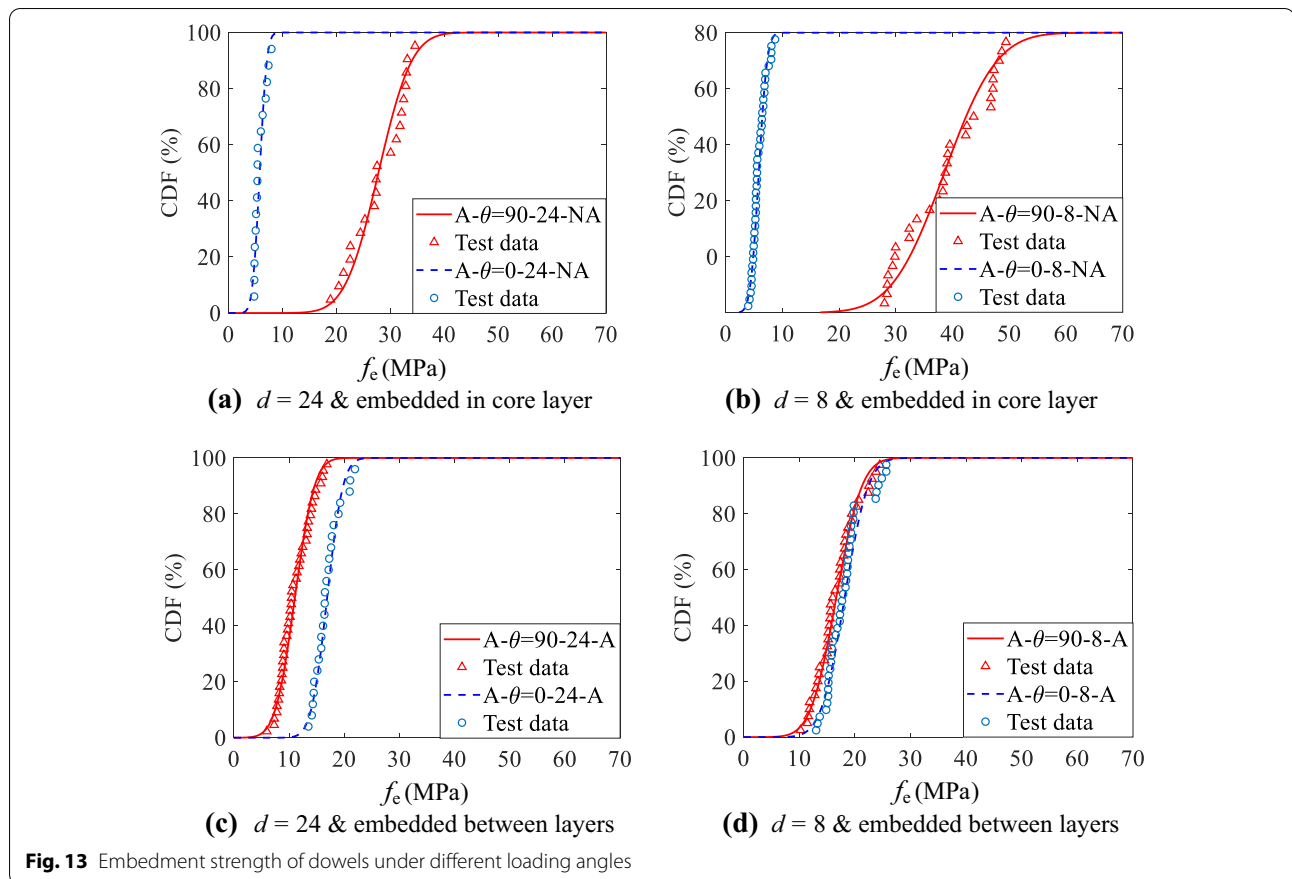


**Fig. 13** Embedment strength of dowels under different loading angles

embedment force. Therefore, the embedment strength of the dowels with a  $\beta$  of 90 degree is higher than that of the dowels with a  $\beta$  of 0 degree.

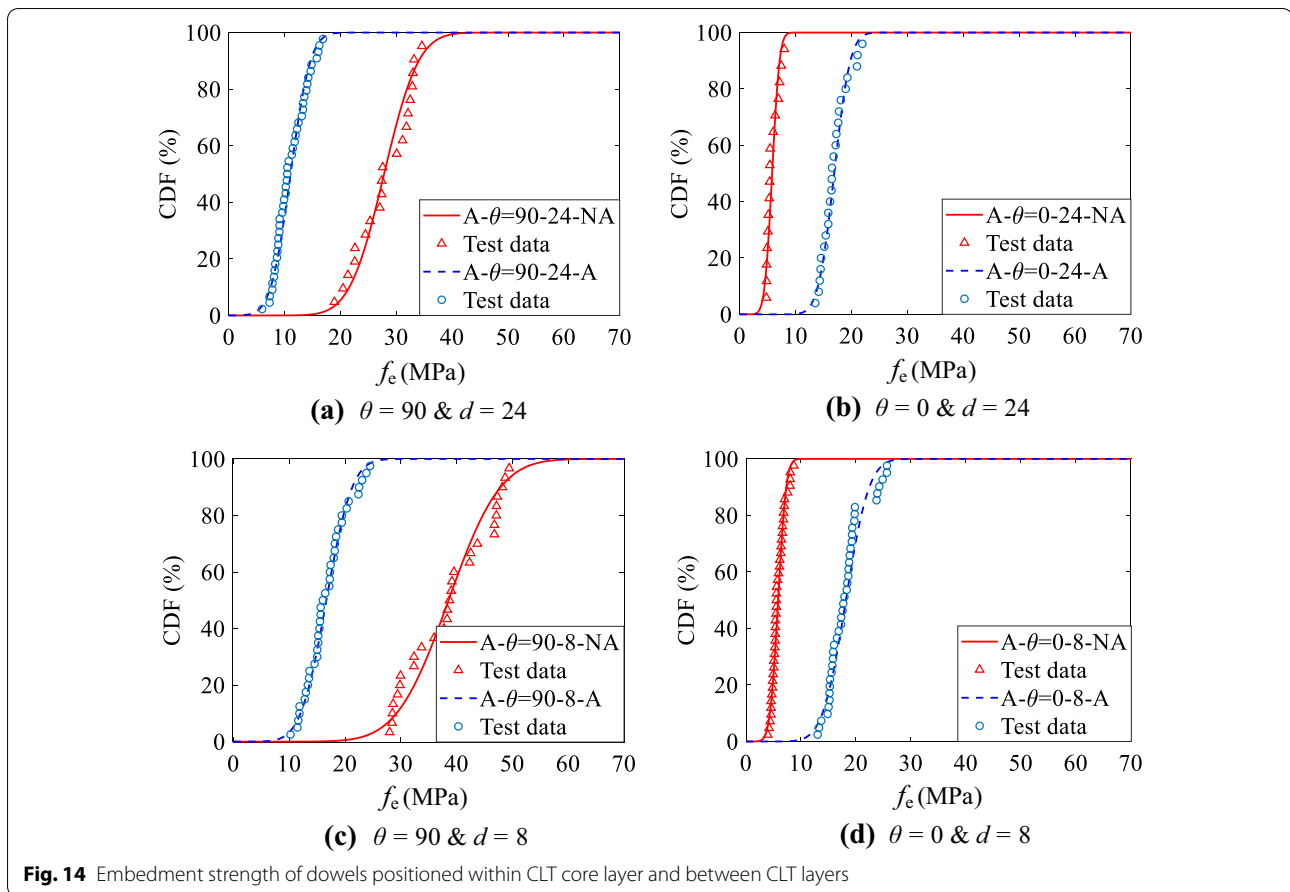
**Gap between lumbers**

For the CLT embedment specimens in the subgroups 9 to 16 with the loading direction perpendicular to the adhesive layer, when the embedment angle  $\beta$  is 90 degree, the gap between the lumbers existing in the embedment position of the dowels can weaken their  $f_e$ . For instance, when the embedment angle is 90 degree and the  $d$  is 8 mm,  $f_{e,ave}$  of the dowels embedded in the gap is 7.67% less than that of the laterally loaded dowels that are not affected by the gap (Table 2), as shown in Fig. 16c. Whereas, when the embedment angle  $\beta$  is 0 degree, namely, the orientation of the dowels is parallel to the grain orientation of the embedment layer, almost no drop can be identified for  $f_e$  of the dowels when the gap exists in their embedment position, as shown in Fig. 16b, d. It might be because when the embedment angle is 90 degree, the gap between the lumbers existing in the embedment position cut off the original continuous wood fibers that pass through the embedment position. It would weaken the force-resisting capacity of the embedment position, which is provided

by the group of the wood fibers passing through the embedment position. By contrast, when the embedment angle is 0 degree, the gap between the lumbers existing in the embedment position does not cut off the wood fibers within the embedment area. Therefore, when the embedment angle  $\beta$  is 90 degree, the gap between the lumbers can weaken the embedment strength. Whereas, when the embedment angle  $\beta$  is 0 degree, the gap between the lumbers has little effect on the embedment strength.

**Verification of the existing design equations**

In this study, the aforementioned Eq. (1) by Uibel and Blab [13–15] and Eq. (3) from the CSA O86 [23] were, respectively, verified, by comparing the average embedment strength predicted by Eqs. (1) or (3) with the average value of the experimental embedment strength. It should be noted that the characteristic embedment strength predicted by Eqs. (2) or (4) was not verified. It is because the characteristic value of the experimental embedment strength obtained based on the short-term load duration (i.e., no more than 15 min) should be adjusted by the load-duration factor, before comparing with the characteristic value of the predicted embedment strength. Whereas, the load-duration factor for the

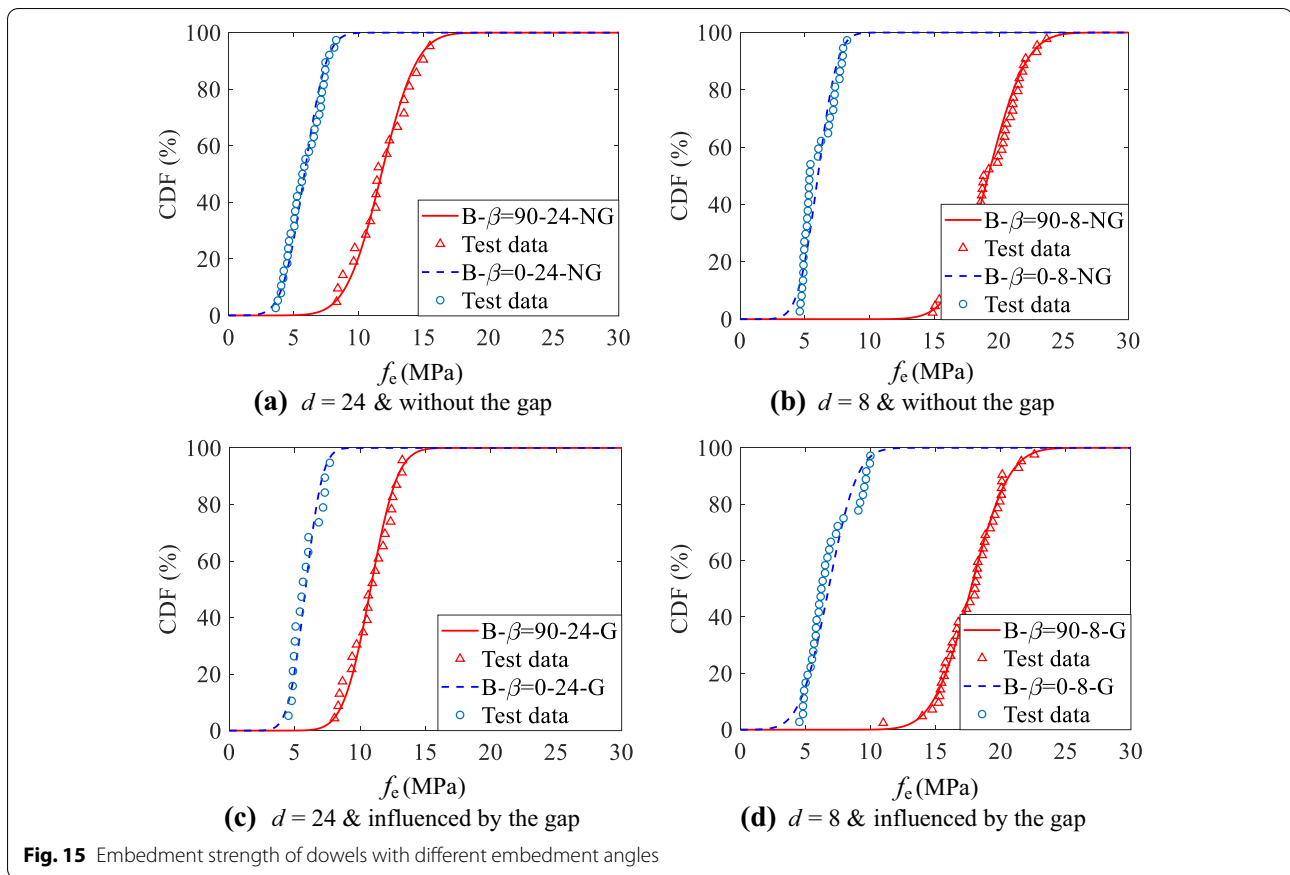


embedment strength of CLT has not been determined, which is dependent on the type of load, the type of engineered wood, the required reliability specified by the domestic codes, etc.

The comparison of the average embedment strength between the experimental results and the predictions based on Eq. (1) is shown in Fig. 17. Around 8.7% of the embedment strength predicted by Eq. (1) are higher than the experimental embedment strength for the specimens in the group A. As for the group B, around 39.8% of the predicted embedment strength are higher than the experimental embedment strength. It is noted that for the four subgroups with a  $\beta$  of 0 degree in the group B, the experimental embedment strength of all the replicates is less than the embedment strength predicted by Eq. (1), as shown in Fig. 17b. It indicates that Eq. (1) is un-conservative for predicting the embedment strength of the specimens with a  $\beta$  of 0 degree.

Compared to Eq. (1) from Uibel and Blab [13–15], the influence of the loading angle relative to the grain orientation of the embedment layer is considered in Eq. (3) from the CSA O86 [23]. The comparison of the average embedment strength between the experimental

results and the predictions based on Eq. (3) is shown in Fig. 18. Around 49.2% of the embedment strength predicted by Eq. (3) are higher than the experimental embedment strength for the specimens in the group A. By contrast, for the specimens in the group B, the ratio of the predicted embedment strength that is higher than the experimental embedment strength is enhanced to 68.3%. Therefore, compared to Eq. (1), Eq. (3) is less conservative for the estimation of the average embedment strength of the dowels inserted in CLT narrow side. For the two subgroups with a  $\beta$  of 0 degree in the group A (i.e., A- $\theta=0$ -8-NA and A- $\theta=0$ -24-NA) and the four subgroups with a  $\beta$  of 0 degree in the group B, the experimental embedment strength of all the replicates is less than the predicted embedment strength. It indicates that Eq. (3) is un-conservative for predicting the embedment strength of the dowels inserted in CLT narrow side with a  $\beta$  of 0 degree. Besides, it is noted that for the subgroups of A- $\theta=90$ -8-A and A- $\theta=90$ -24-A, the average embedment strength is overestimated by Eq. (3), when compared to the average value of the experimental embedment strength, as shown in Fig. 18a.



**Modification of the existing equations for average embedment strength**

The empirical model expressed by Eq. (3) is more complicated compared to the general empirical model expressed by Eq. (1). Therefore, it was determined that necessary modification was conducted based on the empirical Eq. (3) from the CSA O86 [23] for a more accurate prediction on the average embedment strength of smooth dowels inserted in CLT narrow side. The modified empirical model can be expressed by Eqs. (6)–(8), in which, the influencing factors including the embedment position, the loading angle relative to the grain of the embedment layer  $\theta_e$ , and the embedment angle  $\beta$  are considered. Based on the modified Eqs. (6)–(8), the average embedment strength  $f_{\theta,ave,Mod,nar}$  was predicted for the sub-groups 1 to 16, which was then compared to the average value of the experimental embedment strength  $f_{e,ave}$ , as shown in Fig. 19. Statistical comparison of the prediction accuracy was conducted for the existing Eqs. (1) and (3) as well as the modified Eqs. (6)–(8), as listed in Table 4. It is found that the mean absolute error or the absolute percent error based on the modified Eqs. (6)–(8) is much less than that based on the existing Eq. (1) or (3). It suggests that compared to the existing empirical Eq. (1) or

(3), the modified empirical equations can provide a more accurate prediction on the average embedment strength of the smooth dowels inserted in CLT narrow side.

For smooth dowel positioned between CLT layers:

$$f_{\theta,ave,Mod,nar} = \frac{0.9 \times 82\rho_{12}(0.5 - 0.005d)}{0.9 \times 2.27 \sin^2 \theta_e + \cos^2 \theta_e} + \frac{0.9 \times 82\rho_{12}(0.5 - 0.005d)}{0.9 \times 2.27 \cos^2 \theta_e + \sin^2 \theta_e} \quad (6)$$

For smooth dowel positioned within CLT core layer &  $\beta = 90$  degree:

$$f_{\theta,ave,Mod,nar} = \frac{0.9 \times 82\rho_{12}(1 - 0.01d)}{0.9 \times 2.27 \sin^2 \theta_e + \cos^2 \theta_e} \quad (7)$$

For smooth dowel positioned within CLT core layer &  $\beta = 0$  degree:

$$f_{\theta,ave,Mod,nar} = \frac{0.5 \times 82\rho_{12}(1 - 0.01d)}{0.9 \times 2.27 \sin^2 \theta_e + \cos^2 \theta_e} \quad (8)$$

Based on a series of CLT embedment tests conducted by Uibel et al. [14] and Dong et al. [21], the average embedment strength  $f_{e,ave}$  of the fasteners inserted in

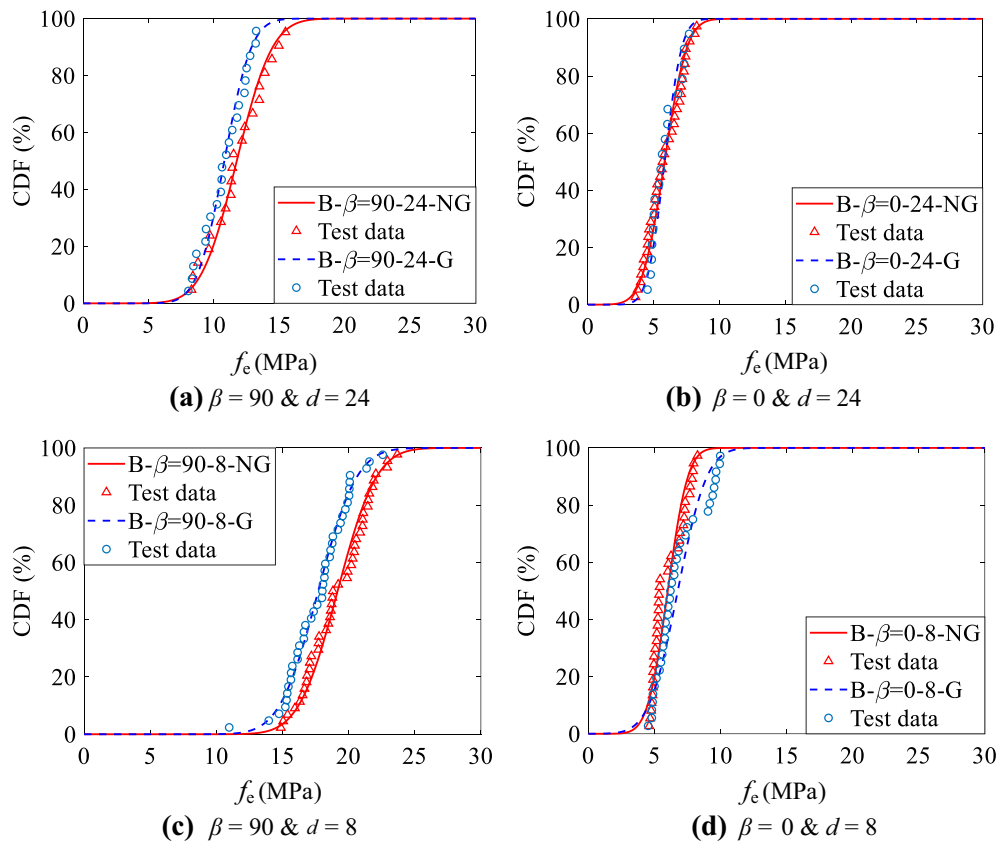


**Fig. 16** Embedment strength of dowels positioned in the gap and without the gap

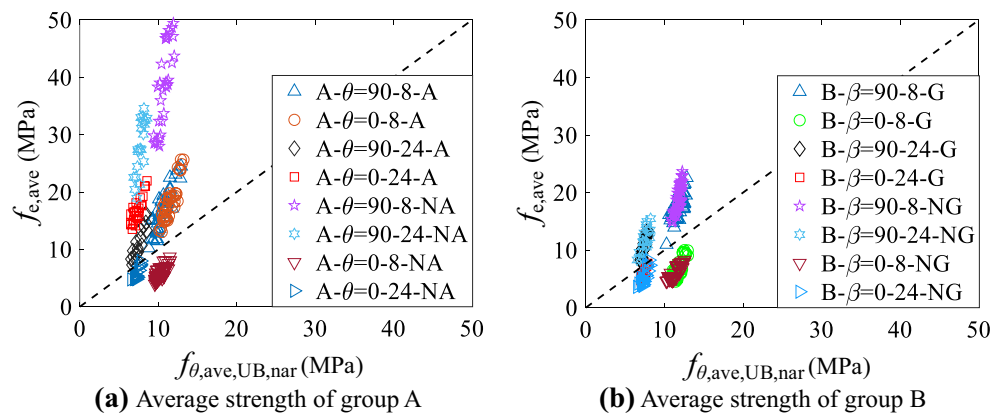


**Fig. 17** Verification of the empirical Eq. (1)

CLT narrow side was obtained. In these studies, both 3-layer CLT and 5-layer CLT were tested, and the  $d$  of the dowel-type fasteners ranged from 8 to 24 mm. The test data from the references [14] and [21] were used to verify the proposed empirical Eqs. (6)–(8) in this study. The

experimental embedment strength  $f_{e,ave}$  from the references and the embedment strength  $f_{\theta,ave,Mod,nar}$  predicted based on Eqs. (6)–(8) are listed in Table 5. It is illustrated that the predictive embedment strength is similar to the experimental embedment strength. It indicates that the

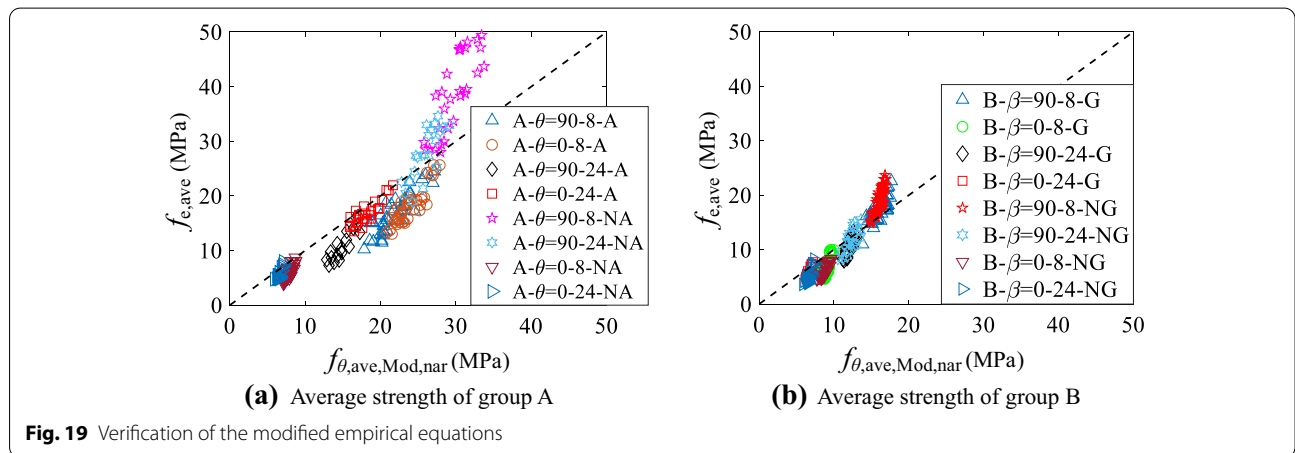
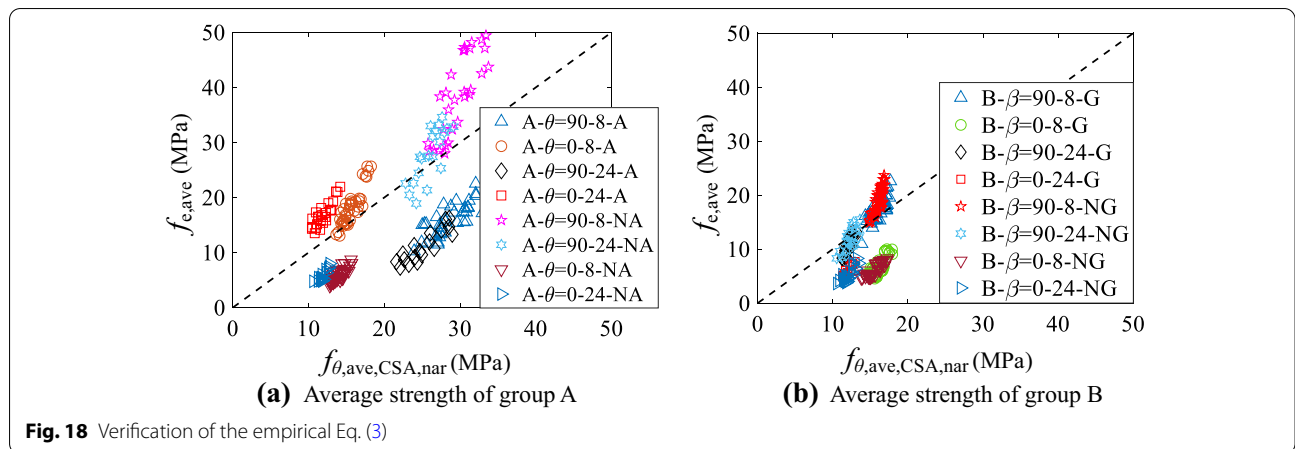


**Table 4** Comparisons of the existing and the modified equations for average strength

Empirical model	Mean absolute error (MPa)	Absolute percent error (%)
Equation (1)	7.1641	49.70
Equation (3)	6.2473	72.40
Equations (6)–(8)	3.1318	22.11

modified Eqs. (6)–(8) are capable of providing a relatively accurate prediction on the average embedment strength of the dowels inserted in CLT narrow side.

**Conclusions**

Based on comprehensive tests on 504 CLT embedment specimens, the embedment strength of the smooth dowels inserted in CLT narrow side was investigated, and the effects of the influencing factors on the embedment strength were analyzed. Besides, the existing

empirical equations for estimating the average embedment strength were validated, and modified equations were proposed for a more accurate prediction on it. The main conclusions are as follows:

- (1) When the loading direction with a loading angle of 90 degree is parallel to the CLT adhesive layer, for the dowels embedded in the core layer and for those embedded between layers, the average embedment strength decreases by 27.89% and by 33.61% with an increase of the  $d$  from 8 to 24 mm, respectively. It is because when the  $d$  increases, the embedment area of the CLT specimens covered by the dowels is enhanced, and more intrinsic defects would be contained. The influence of the embedment length on the embedment strength was not considered, which should be further investigated in the future.
- (2) When embedded between CLT layers, the average embedment strength of the dowels under a  $\theta$  of 90 degree is less than that of the dowels under a loading angle of 0 degree. It is because the CLT with the

**Table 5** Verification of the modified equations based on the test data from the references

Group ID	$\rho_{12}$ (g/cm <sup>3</sup> )	$d$ (mm)	$\theta_e$ (°)	$\beta$	By equation	$f_{\theta,ave,Mod,nar}$ (MPa)	$f_{e,ave}$ (MPa)
A1 from Ref. [14]	0.47	16	90	0°	(8)	7.92	11.75
A2 from Ref. [14]	0.43	16	0	90°	(7)	26.66	32.68
		8	0	90°	(7)	29.20	34.01
B1 from Ref. [14]	0.47	24	90	0°	(8)	7.17	9.40
A5 from Ref. [14]	0.45	12	90	–	(6)	21.76	20.25
		24	90	–	(6)	18.80	17.51
A from Ref. [21]	0.55	12	0	90°	(7)	35.72	37.66
B from Ref. [21]		12	90	90°	(7)	17.48	19.89
C from Ref. [21]		12	90	0°	(8)	10.71	12.55
D from Ref. [21]		12	90	0°	(8)	10.71	13.20

dowels loaded with a  $\theta$  of 0 degree is composed of two longitudinal face layers and one transverse core layer. Its in-plane compressive strength is higher than that of the CLT with the dowels loaded with a  $\theta$  of 90 degree.

- (3) When the loading direction is perpendicular to the adhesive layer, the average embedment strength of the smooth dowels with a  $\beta$  of 90 degree is 85.25–218.96% higher than that of the dowels with a  $\beta$  of 0 degree. It is because when the  $\beta$  is 90 degree, more wood fibers of the embedment layer are subjected to the embedment force.
- (4) When the loading direction is perpendicular to the CLT adhesive layer, in case of a  $\beta$  of 0 degree, almost no drop can be identified for the embedment strength of the dowels when the gap exists in their embedment position. It might be because when the  $\beta$  is 0 degree, the gap between the lumbers existing in the embedment position does not cut off the wood fibers within the embedment area.
- (5) The modified empirical equations can provide a more accurate prediction on the average embedment strength of the smooth dowels inserted in CLT narrow side, compared to the existing empirical equations.

To conclude, the results will be helpful to achieve a more efficient utilization of the dowel-type fasteners and facilitate a more reliable design of the CLT connections. Although CLT layout and connection combinations vary greatly, the proposed empirical model is capable of serving as a potential tool for estimating the embedment strength of dowels inserted in CLT narrow side.

**Abbreviations**

CLT: Cross-laminated timber; COV: Coefficient of variation; SPF: Spruce-pine-fir; LVDT: Linear variable differential transducer;  $\rho_{12}$ : The measured density based on mass and volume of CLT with 12% moisture content;  $\rho_{12,k}$ : The

characteristic density based on mass and volume of CLT with 12% moisture content;  $G$ : The characteristic relative density based on oven-dry mass and volume;  $G_0$ : The measured relative density for the species based on oven-dry mass and volume;  $f_{\theta,ave,UB,nar}$ : The average value of the embedment strength based on equations by Uibel and Blab;  $f_{\theta,k,UB,nar}$ : The characteristic value of the embedment strength based on equations by Uibel and Blab;  $\theta_e$ : The loading angle relative to the grain of the CLT embedment layer;  $\theta$ : The loading angle relative to the grain orientation of the CLT face layers;  $\beta$ : The embedment angle defined as the angle between the orientation of the dowel and the grain orientation of the CLT embedment layer;  $l$ : Embedment length;  $f_e$ : The experimental embedment strength calculated from the force–displacement curve;  $f_{e,k}$ : The characteristic value of the experimental embedment strength;  $f_{e,max}$ : The maximum value of the experimental embedment strength;  $f_{e,min}$ : The minimum value of the experimental embedment strength;  $f_{e,ave}$ : The average value of the experimental embedment strength;  $F_u$ : The ultimate embedment force from tests;  $F_{max}$ : The maximum embedment force from tests;  $f_{\theta,ave,Mod,nar}$ : The average value of the embedment strength based on the modified empirical model; PRF: Phenol resorcinol formaldehyde; CDFs: Cumulative distribution functions.

**Acknowledgements**

Not applicable.

**Author contributions**

WL: writing—original draft, visualization. JO: conceptualization, methodology. XS: conceptualization, supervision, and formal analysis. XH: investigation, data curation. MH: investigation, data curation. ZL: writing—review and editing. All authors read and approved the final manuscript.

**Funding**

The authors gratefully acknowledge the support from National Key R&D Program of China (Grant No. 2019YFD1101001), CSCEC R&D Project (Grant No. CSCEC-2021-Z-40), and National Natural Science Foundation of China (Grant No. 52108242).

**Availability of data and materials**

The data sets used and/or analyzed during the current study are available from the corresponding author on reasonable request.

**Declarations**

**Ethics approval and consent to participate**

Not applicable.

**Consent for publication**

Not applicable.

**Competing interests**

There is no conflict of interests.

**Author details**

<sup>1</sup>China National Organization for Timber Construction Design Standard, China Southwest Architectural Design and Research Institute Co. Ltd., Chengdu 610041, China. <sup>2</sup>Department of Structural Engineering, Tongji University, Shanghai 200092, China.

Received: 5 May 2022 Accepted: 26 July 2022

Published online: 05 August 2022

**References**

- Karacebeyli E, Gagnon S (2019) Canadian CLT Handbook, 2nd edn. FPInnovations, Vancouver
- ANSI, APA PRG 320 (2018) Standard for performance-rated cross-laminated timber. American National Standards Institute/APA-The Engineering Wood Association, APA, Tacoma
- Sun XF, He MJ, Li Z (2020) Novel engineered wood and bamboo composites for structural applications: state-of-art of manufacturing technology and mechanical performance evaluation. *Constr Build Mater* 249:11875–11885
- Izzi M, Casagrande D, Bezzi S, Pasca D, Follesa M, Tomasi R (2018) Seismic behavior of cross-laminated timber structures: a state-of-the-art review. *Eng Struct* 170:42–52
- Li Z, Wang XJ, He MJ (2022) Experimental and analytical investigations into lateral performance of cross-laminated timber (CLT) shear walls with different construction methods. *J Earthq Eng* 26(7):3724–3746
- Oh JK, Hong JP, Kim CK, Pang SJ, Lee SJ, Lee JJ (2017) Shear behavior of cross-laminated timber wall consisting of small panels. *J Wood Sci* 63:45–55
- Ringhofer A, Brandner R, Blab HJ (2018) Cross laminated timber (CLT): Design approaches for dowel-type fasteners and connections. *Eng Struct* 171:849–861
- Sun XF, He MJ, Li Z (2018) Performance evaluation of multi-storey cross-laminated timber structures under different earthquake hazard levels. *J Wood Sci* 64(1):23–39
- Schneid E, de Moraes PD (2017) Grain angle and temperature effect on embedding strength. *Constr Build Mater* 150:442–449
- Yurrita M, Cabrero JM (2018) New criteria for the determination of the parallel-to-grain embedment strength of wood. *Constr Build Mater* 173:238–250
- Van Blokland J, Florisson S, Schweigler M, Ekevid T, Bader TK, Adamopoulos S (2021) Embedment properties of thermally modified spruce timber with dowel-type fasteners. *Constr Build Mater* 313:125517
- Stamatopoulos H, Massaro FM, Qazi J (2022) Mechanical properties of laterally loaded threaded rods embedded in softwood. *Eur J Wood Wood Prod* 80:169–182
- Uibel T, Blab HJ (2006) Load carrying capacity of joints with dowel type fasteners in solid wood panels. In: 39th CIB-W18 Meeting, Florence, Italy, 28–31 August, 2006, Paper No. 39-7-5
- Uibel T, Blab HJ (2013) Joints with dowel type fasteners in CLT structures. In: COSTAction FP1004, Focus Solid Timber Solutions–European Conference on Cross Laminated Timber (CLT). Graz, Austria, 21–22 May, 2013, pp. 119–134
- Uibel T, Blab HJ (2007) Edge joints with dowel type fasteners in cross laminated timber. In: Proceedings of the 44th CIB-W18 meeting, Bled, Slovenia, 28–31 August, 2007, Paper No. 40-7-2.
- Tuhkanen E, Mölder J, Schickhofer G (2018) Influence of number of layers on embedment strength of dowel-type connections for glulam and cross-laminated timber. *Eng Struct* 176:361–368
- Dong WQ, Wang ZQ, Zhou JH, Huang H, Yao Y, Zheng W, Gong M, Shi XY (2020) Embedment strength of smooth dowel-type fasteners in cross-laminated timber. *Constr Build Mater* 233:117243
- Ringhofer A, Brandner R, Blab HJ (2018) Cross laminated timber (CLT): design approaches for dowel-type fasteners and connections. *Eng Struct* 171:849–861
- Gikonyo JW, Schweigler M, Bader TK (2021) A spring model for prediction of the nonlinear embedment load-displacement behavior of dowel-type fasteners in cross-laminated timber. In: World Conference on Timber Engineering 2021, Santiago, Chile, 9–12 August, 2021, Paper No. 174133
- Maia BB, Miotto JL, de Góes JLN (2021) Embedding strength of fully-threaded dowel-type fasteners in cross-laminated timber: an experimental study. *Revista Materia* 26(3):e13054
- Dong WQ, Li Q, Wang ZQ, Zhang H, Lu XL, Gong M (2020) Effects of embedment side and loading direction on embedment strength of cross-laminated timber for smooth dowels. *Eur J Wood Wood Prod* 78:17–25
- EN 1995-1-2 (2004) Eurocode 5: Design of timber structures - part 1–2: general-structural fire design
- CSA O86-14 (2014) Engineering design in wood. CSA Group, Mississauga
- Kennedy S, Salenikovich A, Munoz W, Mohammad M (2014) Design equations for dowel embedment strength and withdrawal resistance for threaded fasteners in CLT. In: Proceedings of the World Conference on Timber Engineering, Quebec, Canada, 10–14 August, 2014.
- NDS (2018) National design specification for wood construction. American Wood Council, Leesburg, p. 2018
- EN 14358:2016 (2016) Timber structures—Calculation and verification of characteristic values. CEN, Brussels
- National Lumber Grades Authority (NLGA) (2010) Standard grading rules for Canadian Lumber. Surrey, Canada
- EN 383 (2007) Timber structures—test methods—determination of embedding strength and foundation values for dowel type fasteners. CEN, Brussels
- Blaß HJ, Uibel T (2007) Tragfähigkeit von stiftförmigen Verbindungsmitteln in Brettsperrholz. Universitätsverlag Karlsruhe, Karlsruhe (In German)
- Xu BH, Jing CK, Bouchaïr A (2021) Experimental analysis of the influence of the fastener type on the embedment strength parallel to the grain in glued laminated timber. *J Mater Civ Eng* 33(2):06020023
- ASTM D5764-97a (2018) Standard test method for evaluating dowel-bearing strength of wood and wood-based products. ASTM International, West Conshohocken
- Santos CL, Jesus AMDP, Morais JLL, Lousada JLPC (2010) A comparison between the EN 383 and ASTM D5764 test methods for dowel-bearing strength assessment of wood: experimental and numerical investigations. *Strain* 46(2):159–174

**Publisher's Note**

Springer Nature remains neutral with regard to jurisdictional claims in published maps and institutional affiliations.

Submit your manuscript to a SpringerOpen® journal and benefit from:

- Convenient online submission
- Rigorous peer review
- Open access: articles freely available online
- High visibility within the field
- Retaining the copyright to your article

Submit your next manuscript at ► [springeropen.com](https://www.springeropen.com)